*Article*

# Environmental Risk Assessment Based on High-Resolution Spatial Maps of Potentially Toxic Elements Sampled on Stream Sediments of Santiago, Cape Verde

**Marina M. S. Cabral Pinto [1,2,3,\*], Eduardo A. Ferreira da Silva [1], Maria M. V. G. Silva [3], Paulo Melo-Gonçalves [4] and Carla Candeias [1]**

[1] GeoBioTec—Geobiosciences, Geotechnologies e Geoengineering Research Center, Geosciences Department, University of Aveiro, Campus de Santiago, 3810-193 Aveiro, Portugal; E-Mails: eafsilva@ua.pt (E.A.F.S.); candeias@ua.pt (C.C.)
[2] CNC Centre-Centre for Neuroscience and Cell Biology, College of Medicine, University of Coimbra, 3004-517 Coimbra, Portugal
[3] Department of Geosciences, Geosciences Centre, University of Coimbra, 3000-272 Coimbra, Portugal; E-Mail: mmvslva@ci.uc.pt
[4] Department of Physics and Centre for Environmental and Marine Studies (CESAM), University of Aveiro, 3810-193 Aveiro, Portugal; E-Mail: pmg@ua.pt

\* Author to whom correspondence should be addressed; E-Mail: marinacp@ci.uc.pt; Tel.: +351-964-332-189.

External Editors: Jose A. Centeno, Robert B. Finkelman and Olle Selinus

**Abstract**: Geochemical mapping is the base knowledge to identify the regions of the planet with critical contents of potentially toxic elements from either natural or anthropogenic sources. Sediments, soils and waters are the vehicles which link the inorganic environment to life through the supply of essential macro and micro nutrients. The chemical composition of surface geological materials may cause metabolic changes which may favor the occurrence of endemic diseases in humans. In order to better understand the relationships between environmental geochemistry and public health, we present environmental risk maps of some harmful elements (As, Cd, Co, Cr, Cu, Hg, Mn, Ni, Pb, V, and Zn) in the stream sediments of Santiago, Cape Verde, identifying the potentially harmful areas in this island. The Estimated Background Values (EBV) of Cd, Co, Cr, Ni and V were found to be above the Canadian guidelines for any type of use of stream sediments and also above the target

values of the Dutch and United States guidelines. The Probably Effect Concentrations (PEC), above which harmful effects are likely in sediment dwelling organisms, were found for Cr and Ni. Some associations between the geological formations of the island and the composition of stream sediments were identified and confirmed by descriptive statistics and by Principal Component Analysis (PCA). The EBV spatial distribution of the metals and the results of PCA allowed us to establish relationships between the EBV maps and the geological formations. The first two PCA modes indicate that heavy metals in Santiago stream sediments are mainly originated from weathering of underlying bedrocks. The first metal association (Co, V, Cr, and Mn; first PCA mode) consists of elements enriched in basic rocks and compatible elements. The second association of variables (Zn and Cd as opposed to Ni; second PCA mode) appears to be strongly controlled by the composition of alkaline volcanic rocks and pyroclastic rocks. So, the second PCA mode is also considered as a natural lithogenic mode. The third association (Cu and Pb; third PCA mode) consists of elements of anthropogenic origin.

---

## 1. Introduction

The study of the effects of the geological environment on human health is the main area of Geomedicine. Natural processes (e.g., weathering, escape of gases and fluids along major fractures in the Earth's crust, and volcanic related activity) release to the environment large amounts of elements. Some elements are macro and micro nutrients for the human alimentary (digestive) supply, and some of these can be harmful to humans, even in small concentrations, e.g., Hg, As, Pb, Sb, Bi, Cd, Ag, Al, Be, Sn [1]. Besides natural factors, human activities, such as agriculture industry, and specifically mining [2,3], enhance the introduction of these elements in the human food chain.

The dispersion of chemical elements in the environment is carried out by sediments, soils and waters, which are the vehicles which link the inorganic environment to life. Variations in its natural chemical composition may cause metabolic changes favouring the occurrence of endemic diseases, such as gout, fluorosis, arsenicosis and Keshan's disease, or conversely may be health promoting [4]. No more than 10%–12% of neurologic diseases have a strict genetic etiology, while the majority of cases has unknown origin [5]. According to Gorell *et al.* [6], environmental and occupational exposure to Mn, Cu, Pb, Fe, Zn, Al, appears to be a risk factor for Parkinson's and Alzheimer's diseases. Several authors [7–13] suggest a correlation between the inhalation and ingestion of Mn and disorders of the nervous central system in rats, primates and humans. The International Agency for Research on Cancer shows that the occupational exposure to chromium [VI] is carcinogenic to humans [14]. This agency also concluded that nickel compounds are carcinogenic to humans and that metallic nickel is possibly carcinogenic to humans.

Environmental exposure to cadmium and lead is associated with alterations in renal function [15] and cadmium and chromium also are related to hypertension and atherosclerosis [16].

Knowledge of the geochemistry of sediments, soils and waters is essential to understand the causes of some endemic diseases and, therefore, contribute to the improvement of the nutritional status of the population living on areas where excess or deficiency of some elements occur, e.g., [17,18]. The determination of geochemical baselines and the geochemical cartography are of major importance because they provide a base framework required by objective and effective methods for addressing environmental concerns [19].

Understanding the abundance and spatial distribution of chemical elements in the near-surface environment of the Earth is critical for fields such as risk-based assessment of contaminated land, agriculture, animal and human health, water quality, land use planning, mineral exploration, industrial pollution, and environmental regulation [20]. National geochemical surveys have been a priority in many countries given the importance and applicability of the resulting geochemical databases, e.g., [21–24]. These surveys provide the natural state of the environment [20,21,25–29] and allow the discrimination between geogenic sources and anthropogenic pollution [19,30–32], which is useful for the determination of environmental impacts of mines [33,34], agriculture [35], geomedicine [4,7], and other fields. Initially, geochemical maps were used for mineral exploration and, therefore, were elaborated at high sample densities (from $1/1$ km$^2$ to $1/25$ km$^2$). Latter, in the late 1960s, the first national low-density geochemical survey was conducted in Africa with a sampling density of $1/200$ km$^2$. Also in this decade, the U.S. Geological Survey project began a national-scale geochemical database, with a density of approximately one site per 6000 km$^2$ [20]. National and even continental surveys conducted in various parts of the world had, generally, sample densities ranging from $1/300$ km$^2$ to $1/18,000$ km$^2$ [24]. Maps of baseline values are especially important in countries like Cape Verde, where intervention limits for near-surface environment are not yet established. Recently, a high-density (approximately $1/3$ km$^2$) geochemical survey was conducted in Santiago Island, Cape Verde archipelago, and the first environmental geochemical atlas was compiled for that region [36]. The field work occurred from 2005 until the beginning of 2008, over six campaigns.

A reliable geochemical baseline can only be established if uncontaminated sites are sampled, e.g., [31,35]. The input of elements into stream sediments resulting from human activities has been growing worldwide, making the finding of uncontaminated stream sediment samples more difficult. Fortunately, the human influence was negligible in Santiago before the sampling survey was conducted for this study (2005–2008), compared to that in developed countries.

In order to better understand the relationships between environmental geochemistry and public health, we conducted an environmental risk assessment using the stream sediments sampling medium in the Santiago Island, Cape Verde, following the guidelines proposed by the International Project IGCP 259 [31]. It is important to highlight that this environmental risk is inferred and not calculated on the basis of possible direct or indirect ingestion pathways (pica, airborne dust, transfer through consumption of plants, *etc.*).

Stream sediments are often a preferred medium for sampling in regional and national geochemical surveys [37] because they provide a composite sample of the catchment area upstream of the sampling point [23], which defines the geochemical background, and tends to integrate all sources of sediment (primary rock and soil) [20]. Therefore, stream sediments are an effective medium to represent the geochemical background.

Environmental risk maps of some potentially harmful metal and metalloids (As, Cd, Co, Cr, Cu, Hg, Mn, Ni, Pb, V, and Zn) are presented in this study, identifying the areas of the island which are potentially problematic concerning human health issues. These risk maps were drawn after an estimation of the geochemical background values of the studied elements.

## 2. Cape Verde Archipelago and Santiago Island: Location and Geology

### 2.1. Settings of the Archipelago of Cape Verde and Santiago Island

The archipelago of Cape Verde composed of 10 islands (Figure 1) is located at the eastern shore of the Atlantic Ocean, 500 km west from Senegal's Cape Verde, in the African western shore, between the latitudes 17°13′ N (Santo Antão Island) and 14°48′ N (Brava Island) and the longitude 22°42′ W (Boavista Island) and 25°22′ W (Santo Antão Island) (Figure 1). The biggest island is Santiago Island (991 km$^2$), located in the southern part of the archipelago and with about half of the country's population [38].

**Figure 1.** The Cape Verde Archipelago and its location in Africa's western coast and Geological cartography of Santiago Island, Cape Verde, modified from [39].
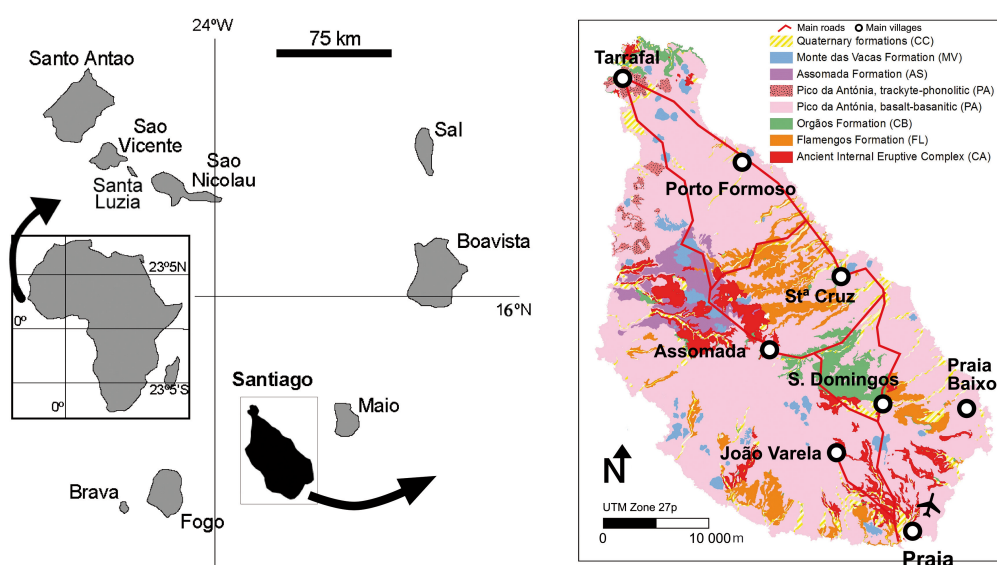


Santiago Island is an elongated NNW-SSE shield-volcano with a maximum length of 54.9 km and a maximum width of 29 km and its maximum altitude reaches 1394 m. The climate is semi-arid, with strong winds during the dry season, and a mean annual precipitation of 321 mm, mainly due to torrential rains, in the wet season [40]. It has 215 km$^2$ of arable area and estimated water resources of $56.6 \times 100$ m$^3$/year at the surface, and $42.4 \times 100$ m$^3$/year underground [41].

### 2.2. Geological Setting of Santiago Island

The major lithological formations of Santiago Island were defined by [39] and [42] (Figure 1), and they show variable geochemistry [36]. The oldest formation, the Ancient Internal Eruptive Complex (CA), is constituted by strongly weathered submarine volcanic products and a dyke complex, which probably represent the submarine edifice-building phase of the island [39,43]. The outcrops of CA are scattered throughout the island (Figure 1), occupying depressions and valleys. There is a wide range of

rock types in the CA, mainly basalts and basanites, but gabbros, alkaline syenites, phonolites, trachytes, breccias and carbonatites also occur.

The Flamengos Formation (FL), with $4.57 \pm 0.31$ Ma [44], is composed of submarine basaltic mantles, with minor hyaloclastic breccias, tuffs, dykes and chimneys. The rocks are limburgites, basanites and basanitoids, with zeolites and carbonates.

The Orgãos Formation (CB) outcrops mostly in the central part of the island but also in the north (Figure 1), and reaches thicknesses of more than 100 m [45]. It is a subaerial and submarine breccia/conglomerate with a sandstone matrix, carbonate and zeolitic cement [39], and probably represents lahars.

The Eruptive Complex of Pico da Antónia (PA) outcrops along more than half of the surface of Santiago Island (Figure 1) and its radiometric age is between $3.25 \pm 0.4$ and $2.25 \pm 0.09$ Ma [44]. It corresponds to the main shield-building stage [43] and is essentially formed by thick sequences of basaltic, submarine and subaerial lava flows [46], with intercalated pyroclastic material. The PA formation also contains dikes, chimneys and endogenous domes of phonolites and trachytes [39]. The lithotypes are essentially ankaratrites, limburgites and basanites, but also nephelinites and olivine-melilitite [42] also occur.

The Assomada Formation (AS) occupies a large depression, is constituted by subaerial almost horizontal, basaltic mantles and some basaltic pyroclastes (Figure 1). The rocks are essentially basanites [42], with gray and reddish colours when weathered.

In Santiago Island, there are 50 scoria cones (the highest reaches 230 m), aligned in the NW-SE direction (Figure 1), constituted by basaltic pyroclastic material and small subordinated flows $(1.13 \pm 0.03$ Ma) [44]. They mark the last volcanic episodes in Santiago Island and were named by Serralheiro (1976) as the Monte das Vacas Formation (MV). The loosely aggregated pyroclasts are exploited for construction, promoting gullies and landslides on the flanks due to erosive action of the water during intense rainfall episodes.

The Quaternary Formations (CC) have a small spatial representation (Figure 1), outcropping in the valleys and close to the shore. They are ancient and modern alluvium, torrent deposits, sand dunes and marine beaches deposits. The terraces reach altitudes of about 100 m.

## 3. Materials and Methods

### 3.1. Sample Collection and Treatment

Between 2005 and 2008, 337 stream sediments composite samples were collected (0–15 cm) across the Santiago Island at a density of ~1 site per 3 km$^2$. Sampling locations were identified using a global positioning system (GPS) and the sampling sites were chosen to be as uncontaminated as possible. Therefore, locations affected by pollution, such as locations near factories or heavy traffic roads and arable soils, were avoided. Given the mountainous topography of Santiago Island and its poor road network, sampling sites are somewhat unevenly distributed.

On each site the composite sample (~1 kg) was obtained by collecting five points, spaced approximately 50 m along the water course. Fresh samples were contained in plastic bags and taken to a laboratory for posterior analyses. Field duplicate samples were taken at every 10 sites, yielding field

duplicates for 26 locations evenly distributed over the island, which will be used in the Analysis of Variance described in Section 3.3.

All samples were air-dried at ~20 °C and visible pebbles were removed. Stream sediments were then sieved to <2 mm, being this fraction used for all analyses. A 10 g split of the retained stream sediments was milled in an agate mill to <0.074 mm for chemical analysis.

*3.2. Chemical Analysis*

The chemical analysis was performed at ACME Analytical Laboratories, Ltd., Vancouver, Canada and according to the laboratory standards methods and QA/QC and protocols. Sample duplicates were analyzed to access precision. Individual samples were digested in *aqua regia* and analysed by inductively coupled plasma-mass spectrometry (ICP-MS) for As, Cd, Co, Cr, Cu, Hg, Mn, Ni, Pb, V, and Zn. Digestion with *aqua regia* is a method of chemical attack more commonly used in environmental studies, than mixtures with HF acid or $HClO_4$ [31]. This type of attack is effective in removing the more mobile elements normally associated with clay minerals, organic matter and other secondary minerals [47–49]. It completely dissolves most of the sulphides, oxides, clay minerals and secondary minerals formed during pedogenesis and other exogenous processes, but most silicate minerals are not dissolved. The samples sent for analysis were randomly numbered in order to remove any systematic relationship between the analysis order and the geographic location, following the recommendations of [31].

*3.3. Analytical Quality Control*

The data resulting from the chemical analysis of the elements was subjected to several data quality tests in order to determine which elements have reliable data to be interpreted by subsequent statistical analysis. The criteria used were: (i) at least 70% of the observations with content greater than the detection limit; (ii) accuracy and precision, quantified by analytical duplicates, having relative standard deviation lower than 10%; and (iii) spatial geochemical variance ($\sigma_G^2$) significantly representative, at a 0.01 significance level, of the spatial total observed variance ($\sigma_T^2$) quantified by an Analysis of Variance using field duplicates sampled at 26 locations evenly distributed over the island.

This Analysis of Variance consists of partitioning the spatial total observed variance ($\sigma_T^2$) into the spatial geochemical variance ($\sigma_G^2$) and the variance associated to errors due to field sampling and chemical analysis ($\sigma_{SA}^2$):

$$\sigma_T^2 = \sigma_G^2 + \sigma_{SA}^2 \tag{1}$$

Each population variance, $\sigma^2$, is estimated by the corresponding sample variance $s^2$:

$$s_T^2 = s_G^2 + s_{SA}^2 \tag{2}$$

where

$$s_T^2 = \frac{1}{N-1}\sum_{n=1}^{N}(X_{1i} - \overline{X}_1)^2 \tag{3}$$

and

$$s_{SA}^2 = \frac{1}{N} \sum_{n=1}^{N} \frac{(X_{1i} - X_{2i})^2}{2} \tag{4}$$

Here, $X_{1i}$ is the concentration observed at the $i$th sampling point and $X_{2i}$ is the concentration at the corresponding field duplicate; $N = 26$ is the number of sampling points (degrees of freedom) and the overbars represent spatial average operators.

Note that the variability of the observed data is $s_T^2$, thus the spatial geochemical variability, $s_G^2$, can only be represented by the total variability, $s_T^2$, if $s_{SA}^2 \ll s_T^2$. To address this issue the following hypothesis test is performed:

$$H_0 : \sigma_{SA}^2 = 0 \; \textit{vs.} \; H_1 : \sigma_{SA}^2 > 0 \tag{5}$$

with the following test statistic

$$F = \frac{s_{SA}^2}{s_T^2} \tag{6}$$

which has a Fisher distribution with $N$ and $N-1$ degrees of freedom, *i.e.*, $F \sim F_{(N, N-1)} = F_{(26, 25)}$. Thus, for each geochemical element, the null hypothesis is rejected at a 1% significance level if $F > 2.589$. The null hypothesis was not rejected for all elements used in this work, meaning that the spatial geochemical variance can be estimated by the observed spatial variance. Moreover, criteria (i) and (ii) were also respected by all these elements.

### 3.4. Estimated Background Value and Statistical Analysis

The methodology followed in this work to determine the Estimated Background Value (EBV) of each metal at each sampling site ($n = 337$) followed the guidelines of the IGCP 259 project, which state that the stream sediments of these sites must be as uncontaminated as possible. The mapping of the EBVs was performed by ordinary kriging using a theoretical model of spatial continuity fitted to the experimental variograms calculated for each element. Cross validation was carried out for each interpolated variable to assess if the fitted model was suitable for the experimental variogram. The root-mean-square error (RMSE) was used to measure the differences between values predicted by the model and the actual values. RMSE ranges from 0 to infinity, with 0 corresponding to the ideal model. Another measure of error, the mean absolute error (MAD) which is less affected by the presence of outliers, is also presented in Table 1.

Please note that the EBV maps are not shown in this work because of space constraints. Nevertheless, the variographic model of each element used for the mapping of the associated Environmental Risk Index (ERI) is described in Section 3.5.

The Estimated Background Value (EBV) at each sampling site was calculated as the median of the data set limited by the Tukey Range: ($P_{25} - 1.5 \times (P_{75} - P_{25})$, $P_{75} + 1.5 \times (P_{75} - P_{25})$) [50]. The Tukey Range filters out possible outliers and is sometimes referred to as the Non-Anomalous Range.

**Table 1.** Parameters of the theoretical models of spatial continuity fitted to the experimental variogram of Co, Cr, Cu, Ni, V, PC1, and PC2.

| ID | Model | Main Direction | $C_0$ | $C_1$ | Length | Anisotropy Ratio | RMSE | MAD |
|----|-------|----------------|-------|-------|--------|------------------|------|-----|
| Co | exponential | 0 | 30 | 150 | 4,000 | 1.27 | 2.38 | 1.58 |
| Cr | exponential | 45 | 2,100 | 1,900 | 2,000 | 1.64 | 3.45 | 2.01 |
| Cu | exponential | 0 | 160 | 200 | 5,000 | 1.22 | 1.05 | 0.98 |
| Ni | exponential | 30 | 2,600 | 2,800 | 3,500 | 1.83 | 4.82 | 2.99 |
| V | exponential | 0 | 1,200 | 600 | 4,000 | 1.98 | 3.56 | 2.33 |
| PC1 | exponential | 90 | 7,000,000 | 9,000,000 | 5,000 | 1.36 | 2.53 | 1.87 |
| PC2 | exponential | 90 | 1,000,000 | 7,500,000 | 2,000 | 1.23 | 1.95 | 1.54 |

Notes: ID: Variable; Model: theoretical model fitted to the experimental variogram; $C_0$: nugget effect; $C_1$: sill for the structure; Length: major range in meters; Anisotropy ratio: Geometrical Anisotropy = major axis/minor axis; RMSE: root-mean-square error; MAD: mean absolute deviation.

A Principal Component Analysis (PCA) was also performed using the correlation matrix, and the number of retained Principal Components (PCs) was objectively determined using the scree graph as follows: the retained modes are those whose eigenvalues decrease sharply. The retained PCs were mapped using the same methodology used in the EBVs' mapping.

Some authors address the question of closure and non-normality when performing a PCA on compositional data [51]. The dataset used in this work is a compositional dataset but it is not a closed one since the data is expressed in its original units and it was not normalized to a constant. Therefore, any logarithmic transformation was performed prior to PCA. The distribution of the data was considered to be approximately Normal due to the Central Limit Theorem and the fact that the concentration of each element at a particular sampling point was computed as the average of the concentrations at five near points. A correlation-based PCA was performed (*i.e.*, the eigenvalues and eigenvectors were computed from the correlation matrix of the original data) instead of a covariance-based PCA because the variables are concentrations of different geochemical elements.

The EBVs' and the PCs' maps were prepared following the recommendations of [31]. The color maps were interpolated by ordinary kriging, based on 337 sites and using a theoretical model of spatial continuity fitted to the experimental variogram calculated for each variable (metal EBV or PC). The parameters of the theoretical models of spatial continuity fitted to the experimental variogram, and the RMSE and MAD values are presented in Table 1.

The color maps were plotted using a color scale classified in eight classes, according to percentiles: [Minimum–$P_{10}$]; [$P_{10}$–$P_{25}$]; [$P_{25}$–$P_{50}$]; [$P_{50}$–$P_{75}$]; [$P_{75}$–$P_{90}$]; [$P_{90}$–$P_{95}$]; [$P_{95}$–$P_{97.5}$]; [$P_{97.5}$–Maximum], where $P_x$ is the *x*th percentile value.

Although the EBV of an element may have a considerable spatial variability, and can, thus, be presented by distribution maps, policy makers usually prefer a single value representative of an entire country or region. Because of this, we determined an EBV representative of the entire Santiago Island (EBV-S) and one EBV representative of each one of its geological formations (EBV-XX where XX are the initials of a particular geological formation). The EBV-S was calculated as the median of the data set limited by the Tukey Range. Each EBV-XX was calculated as the EBV-S, with the difference that the dataset used in the calculations consists of only those sampling points that are located in the XX geological formation.

*3.5. Environmental Risk Assessment*

The concentration of some metals in some areas of the island may be too high for "all types of property uses", according to the Canadian legislation. Therefore, this issue is assessed in this section by means of numeric measures of these environmental risks. For each element, the Environmental Risk Index (ERI) for all types of property uses is quantified by ERI(s) = C(s)/P, where C(s) is the element content observed at sampling site s, and P represents the legislated permissive level of that element, according the Canadian Legislation [52]. The permissible level is, by definition, the element concentration in the stream sediment medium above which the stream sediment is considered to be unsafe for some purpose. We choose the Canadian Guidelines for all types of property uses as the permissible level. Note that the Canadian legislation provides no values for V. So, we used the target value of the Italian guidelines for public/private green areas and residential sites [53].

The procedure used to interpolate and map the ERI fields was the same used for either the EBV or the PC fields. Particularly, the variographic model used for the ERI of an element is the same determined for that element. For the PCs, a new variographic model was determined using the same procedure. These ERI fields indicate where a particular element is above the permissible level, according to the legislation for its use purposes.

## 4. Results and Discussion

*4.1. Estimated Background Values*

Descriptive statistics including the standard deviation (SD), skewness (Skew), kurtosis (Kurt), coefficient of variation percent (CV%), minimum (Min), maximum (Max) and the range of the analyzed metals concentrations along with the EBV-S of Santiago Island were calculated and listed in Table 2.

In order to further explore the relationships between the spatial distribution of the metal contents and the geological formations, the EBV-XX values were calculated. Please remember that an EBV-XX is the estimated background value of a particular metal in the stream sediments collected from a XX geological formation of the Santiago Island (Table 3).

According to Table 3, stream sediments from the Ancient Complex (CA) show high Cr, V, and also Mn. Stream sediments from Flamengos Formation (FL) have high Cu and low Pb concentrations. Órgãos Formation (CB) shown stream sediments with high values of Cu, and low values of Mn and Zn. Stream sediments from Pico da Antónia Formation (PA) have high Co, Cr, Ni and V, and low Zn concentrations. The stream sediments from Assomada Formation (AS) presented high Cd, Mn, Pb and Zn, and low Co, Cr, Cu and Ni (and also V), while the samples collected from the MV formation stands out from the other stream sediment samples by its higher Cd, Hg, As, Pb and Zn concentrations. The sediments of this geological formation are scarce in Cu and V. The Quaternary Formation stream sediments samples are also enriched in As but have low Zn contents. Alluvium samples have high Cr and Ni contents. All these results are in line with those obtained from the comparison of the EBV maps with the geological cartography.

**Table 2.** Statistical As, Cd, Co, Cr, Cu, Hg, Mn, Ni, Pb, V, and Zn variables analysed, interval ranges, and the baseline values (EBV-S) of metals from the stream sediments of Santiago Island ($n = 337$). Values expressed in mg·kg$^{-1}$.

| Var | Min | Med | Me | Max | SD | CV | Sk | Krt | P5–P95 | Tukey Range | EBV-S |
|---|---|---|---|---|---|---|---|---|---|---|---|
| As | 0.3 | 0.3 | 0.6 | 7.2 | 0.62 | 1.07 | 5.18 | 43.79 | 0.3–1.6 | 0.3–1.4 | 0.25 |
| Cd | 0.05 | 0.10 | 0.14 | 1.00 | 0.09 | 0.64 | 3.82 | 30.16 | 0.05–0.30 | 0.05–0.35 | 0.10 |
| Co | 3.1 | 44.7 | 45.1 | 139.9 | 13.86 | 0.31 | 1.21 | 7.79 | 26.4–66.1 | 15.8–73.4 | 44.65 |
| Cr | 8.0 | 114.0 | 123.7 | 463.1 | 68.03 | 0.55 | 1.49 | 4.48 | 20.0–251.5 | 8.0–264.0 | 111.00 |
| Cu | 3.2 | 48.8 | 48.6 | 141.6 | 17.99 | 0.37 | 0.52 | 2.38 | 17.6–77.8 | 9.4–87.6 | 48.70 |
| Hg | 0.01 | 0.01 | 0.01 | 0.08 | 0.01 | 0.74 | 2.13 | 7.24 | 0.15–0.54 | 0.07–0.61 | 0.26 |
| Mn | 197.0 | 1191.0 | 1259.9 | 4210.0 | 441.65 | 0.35 | 2.07 | 8.87 | 737.1–2043.5 | 255.1–2162.1 | 1182.00 |
| Ni | 6.8 | 155.2 | 160.5 | 477.0 | 76.02 | 0.47 | 0.50 | 1.13 | 21.3–286.2 | 6.8–337.5 | 152.85 |
| Pb | 1.4 | 3.9 | 5.2 | 81.4 | 6.61 | 1.26 | 7.53 | 70.27 | 2.0–10.1 | 1.4–10.1 | 3.80 |
| V | 24.0 | 160.0 | 161.0 | 372.0 | 45.68 | 0.28 | 0.64 | 2.57 | 92.4–237.3 | 50.5–262.5 | 159.00 |
| Zn | 15.0 | 81.0 | 82.7 | 189.0 | 19.14 | 0.23 | 1.23 | 5.35 | 57.0–111.0 | 34.0–130.0 | 81.00 |

Notes: Min: minimum; Med: median; Me: Mean; Max: maximum; SD: standard deviation; Sk: skewness; Krt: kurtosis; CV: variation coefficient; P5–P95: the interval limited by the 5th and 95th percentile values; Tukey Range [50] or Non-Anomalous range: $P_{25} - 1.5 \times (P_{75} - P_{25}) - P_{75} + 1.5 \times (P_{75} - P_{25})$; EBV-S (Estimated Background Value for Santiago): the median of the data limited by the Tukey Range.

**Table 3.** Estimated Background Values (EBV-XX) of As, Cd, Co, Cr, Cu, Hg, Mn, Ni, Pb, V, and Zn in the stream sediments of different geological formations in Santiago Island, Cape Verde.

| Variable | EBV-CA ($n = 41$) | EBV-FL ($n = 21$) | EBV-CB ($n = 28$) | EBV-PA ($n = 118$) | EB-AS ($n = 15$) | EBV-MV ($n = 18$) | EBV-CC ($n = 9$) | EBV-AL ($n = 87$) |
|---|---|---|---|---|---|---|---|---|
| As | 0.3 | 0.3 | 0.3 | 0.3 | 0.3 | 0.6 | 0.7 | 0.3 |
| Cd | 0.10 | 0.10 | 0.10 | 0.10 | 0.20 | 0.20 | 0.10 | 0.10 |
| Co | 43.6 | 41.3 | 40.3 | 48.8 | 35.8 | 42.6 | 42.2 | 44.9 |
| Cr | 116.0 | 112.5 | 99.0 | 122.5 | 20.5 | 76.0 | 93.5 | 119.3 |
| Cu | 53.8 | 57.6 | 56.7 | 46.6 | 26.4 | 34.2 | 47.4 | 48.9 |
| Hg | 0.01 | 0.01 | 0.01 | 0.02 | 0.02 | 0.03 | 0.01 | 0.02 |
| Mn | 1199 | 1036 | 980 | 1328 | 1612 | 1423 | 1027 | 1157 |
| Ni | 126.7 | 139.1 | 145.1 | 168.1 | 20.1 | 104.1 | 148.9 | 164.1 |
| Pb | 3.6 | 2.5 | 3.3 | 4.7 | 6.6 | 6.0 | 4.1 | 3.4 |
| V | 166.0 | 157.5 | 148.0 | 167.0 | 153.0 | 131.0 | 147.0 | 156.0 |
| Zn | 86.5 | 80.0 | 76.5 | 76.0 | 99.0 | 88.0 | 73.5 | 81.0 |

Notes: CA: Ancient Intern Eruptive Complex; FL: Flamengos Formation; CB: Órgãos Formation; PA: Pico da Antónia Formation; AS: Assomada Formation; MV: Monte das Vacas Formation; CC: Quaternary Formations; AL: Alluvium. Highest chemical element contents in bold and lowest chemical elements contents with gray highlight.

## 4.2. Multivariate Statistical Analysis

In order to confirm the link between the EBV classes with the geological spatial distribution, a correlation-based PCA was also conducted (see Section 3.4). Using the scree graph (Figure 2a) it was

decided to retain three modes, accounting for 61.02% of the total variance (Figure 2b). Based on the biplots show in Figure 2c, the elements can be assembled into the first three principal vectors (PVs), as follows:

**Figure 2.** (**a**) Scree graph and (**b**) Cumulative Explained Variance of the first 11 PCA (Principal Component Analysis) modes. Red circles are drawn for the three retained components; (**c**) Biplot of PV2 *vs.* PV1 and (**d**) PV3 *vs.* PV1.
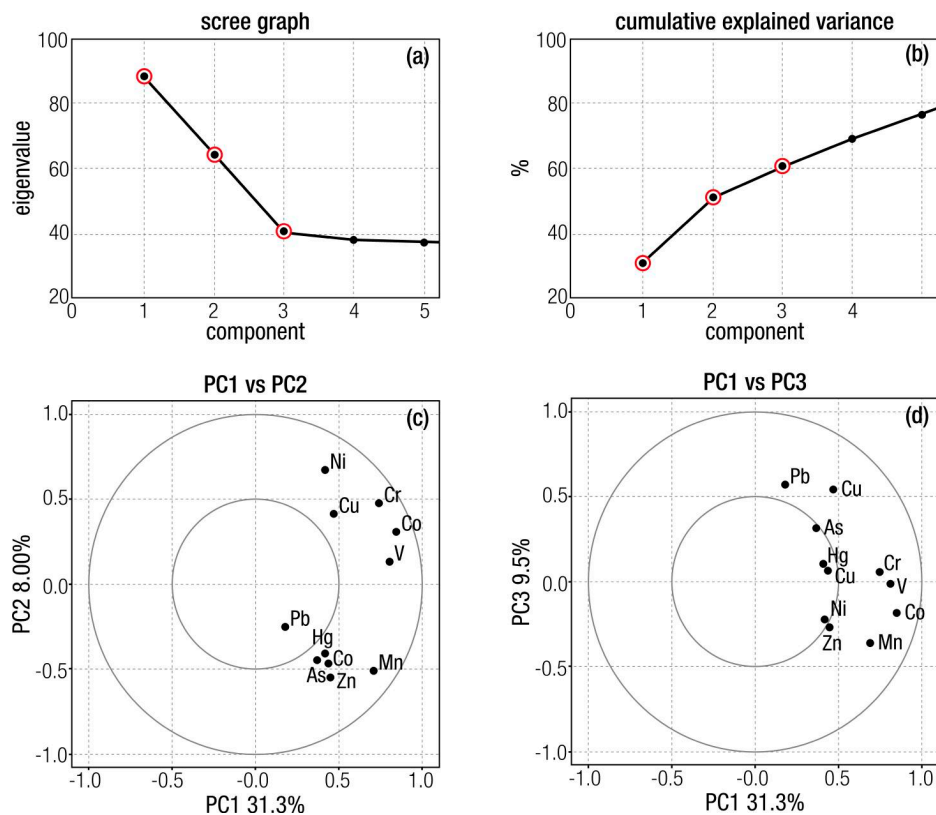


PV1: association of Co, V, Cr, and Mn, displaying high loadings: 0.839, 0.798, 0.732, and 0.686, respectively. The metal association in first PCA mode clearly shows the influence of a lithology rich in siderophile elements (Co, Cr), typical of basic rocks and also the presence of its typical minerals [36], such as pyroxene (V), olivine and serpentine (Co, Cr, Ni). These four elements may exist together in soil and also in stream sediment parent materials, as the weathering products of the exposed bedrocks. Soils (and stream sediments) developed from basic and ultramafic rocks are usually enriched in Ni, Cr and Co [54]. This first factor is then assumed as a natural lithogenic factor.

PV2: Zinc and Cd are associated in the second mode (PV2/PC2), with high negative loadings, −0.558 and −0.513, respectively, in opposition to the element Ni with a strong high positive loading, 0.675. Zinc and Cd are highly associated with pyroclastic deposits of Monte das Vacas Formation. Niquel also shows a positive high value, 0.675, in PC2, leading to the assumption that this metal association primarily shares a natural source feature.

PV3: consists of Cu and Pb association, with the loadings of 0.546 and 0.583, respectively. This mode apparently reflects the influence of anthropogenic sources, namely the possible use of fertilizers and/or pesticides containing Cu and Pb, and/or batteries, particularly at the relatively populous regions, such as Praia, Assomada, Tarrafal and corresponding riversides that can result in the high element loading. These areas pose a potential health risk. Also, the lack of a relationship between these metals and the geological

formations induces a link to an anthropogenic source. In fact, the geological formations where Pb concentrations are higher correspond to the geological formations where Cu contents are lower and *vice versa* (e.g., Assomada and Monte das Vacas formations).

The PV1, PV2 and PV3 loadings (Figure 2) account for 31.28%, 20.28% and 9.47% of the total variability, respectively.

When comparing the spatial distribution of the PCs with the geological formations (Figure 3), it is possible to identify a light relationship between them. The association in PC1 displays the influence of a rich lithology in siderofile elements, typical of basic rocks and the presence of minerals such as pyroxene, amphibole, olivine and serpentine, as referred to previously. PC1 is linked with the basaltic-basanite rocks from the PA Formation, contrarily to the Flamengos (FL) and AS Formations; The metal association in PC2, with Zn and Cd (and As), is associated mainly to the pyroclastic rocks of Monte das Vacas, opposed in sign to Ni, which enters in the structure of the basaltic rocks typical minerals, such as serpentine (Co, Cr, Ni). PC3 apparently reflect the influence of the anthropogenic sources, having no relation with the geological cartography.

**Figure 3.** Spatial distribution of PC1 and PC2. The geological map of Figure 1 is shown in the last panel for easier comparison with the PC spatial fields.
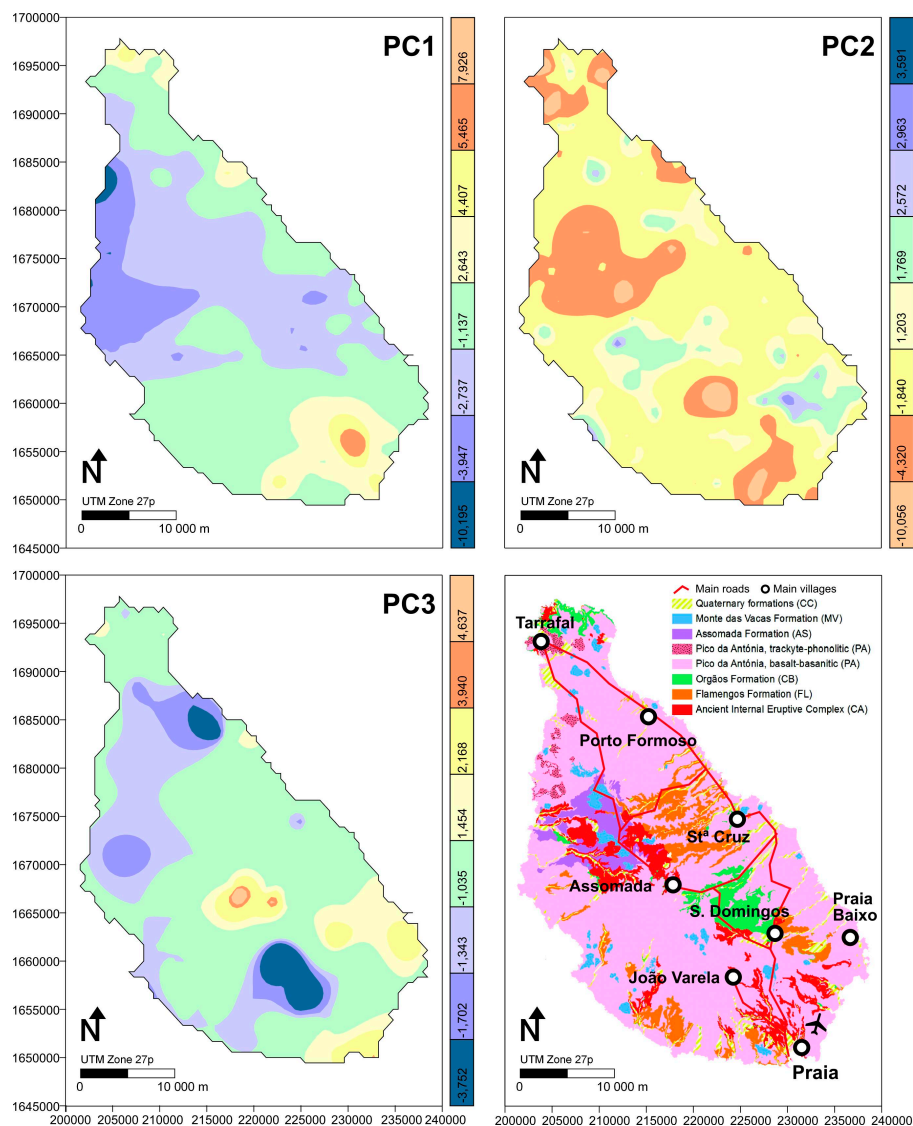
*4.3. Environmental Risk Assessment*

Before analysing the ERI fields, the comparison of the EBV-S of each studied metal in the stream sediments of Santiago Island and the international values legislated as dangerous for certain uses (guideline values), is given in Table 4.

The EBV-S of Cd, Co, Cr, Ni and V are above the Canadian guidelines for stream sediments (for any use) and above the target values of Dutch [55] and United States [56] guidelines. Numerical sediment quality guidelines for freshwater [57] are commonly used to identify sediments that are likely to be toxic to sediment-dwelling organisms. The Probable Effect Concentrations (PEC) quotients allowed to assess the sediments that contain complex mixtures of chemical contaminants (Table 4). The PEC, above which harmful effects are likely in sediment dwelling organisms were compared for As, Cd, Cr, Cu, Hg, Ni, Pb, and Zn. The EBV-S of Cr and Ni were found to be above the Probable effect level (PEL) [58], the Severe effect level (SEL) [59] and the Toxic effect threshold (TET) [60], as shown in Table 4.

Figure 4 shows the ERI maps each element for all types of property uses. Only the ERI maps of the elements that present regions with values above the unit (*i.e.*, above the legislated permissible values) are shown (Figure 4). These elements are Co, Cr, Cu, Ni and V. The Zn map is not shown because it has ERI > 1 only at six sample locations. These metals are precisely those with higher loadings in PV1 and PV2 (Ni), which revealed to be of natural origin in Santiago island.

**Table 4.** Estimated Background Values of harmful elements from the stream sediments of Santiago (EBV-S), admissible levels (in mg·kg$^{-1}$) in stream sediments according to the Ontario, Dutch and United States guidelines, and the numerical sediment quality guidelines for freshwater, including their probable effect concentrations (PEC).

| EBV-S | | Canadian Guidelines | Dutch Guidelines | United States [56] | Numerical Sediment Quality Guidelines for Freshwater Ecosystems |
|---|---|---|---|---|---|
| | | **All Types of Property Uses** | **Target Values** | **Mean Values** | **Probable Effect Concentrations: PEL; SEL; TET** |
| As | 0.60 | 6 | 29 | 3.9 | 17; 33; 17 |
| Cd | 0.91 | 0.6 | 0.8 | - | 3.53; 10; 3 |
| Co | 46.4 | 50 | 9 | 9.1 | -; -; - |
| Cr | 118 | 26 | 100 | - | 90; 110; 100 |
| Cu | 50.8 | 16 | 36 | 14.2 | 197; 110; 86 |
| Hg | 0.02 | 0.2 | 0.3 | - | 0.486; 2; - |
| Mn | 1293 | - | - | 760 | -; -; - |
| Ni | 136.1 | 16 | 36 | 15.1 | 36; 75; 61 |
| Pb | 5.00 | 31 | 85 | 14.1 | 91.3; 250; 170 |
| V | 169 | 90 * | - | 81.1 | -; -; - |
| Zn | 79 | 120 | 140 | 62.9 | 315; 820; 540 |

Notes: PEL: Probable effect level; dry weight [58], in [57]. SEL: Severe effect level; dry weight [59], in [57]. TET: Toxic effect threshold; dry weight [60], in [57]. * Italian legislated value for public/private greens areas and residential sites [53].

**Figure 4.** Environmental Risk Index (ERI) of some metals for all types of property uses. The geological map of Figure 1 is shown in the last panel for easier comparison with the ERI spatial fields.
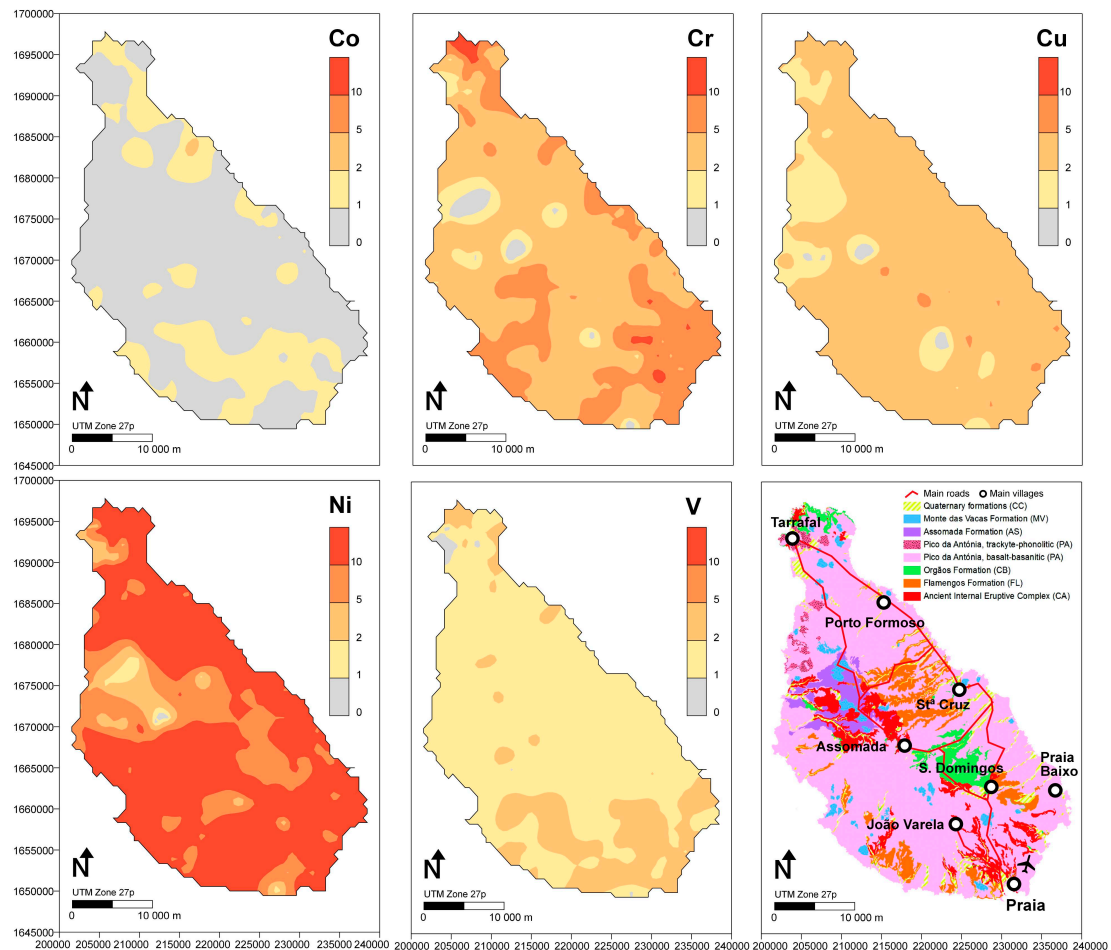


## 5. Conclusions

A clear chemical characterization of the stream sediments in different geological formations is difficult, since the chemical composition of each sampling point represents the chemical composition of the entire area upstream, covering different geological formations. Despite this constraint, the EBV spatial distribution of the metals and the results of PCA allowed establishing relationships between the EBV maps and the geological formations. Furthermore, it is important to emphasize that the stream lines in Santiago have a negligible water flow.

The first two PCA modes indicate that heavy metals in Santiago stream sediments are mainly originated from weathering of underlying bedrocks. The first metal association (Co, V, Cr, and Mn; first PCA mode) consists of elements enriched in basic rocks and compatible elements. These elements are related to pyroxene, amphibole, and olivine minerals that were found in Santiago stream sediments [61].

The second association of variables, Zn and Cd as opposed to Ni (second PCA mode), appears to be strongly controlled by the composition of alkaline volcanic rocks and pyroclastic rocks. The K-feldspar, zircon, pyroxene, amphibole, and olivine are examples of minerals responsible for this association [36,61]. So, the second PCA mode is also considered as a natural lithogenic mode. The third association (third PCA mode: Cu and Pb) consists of elements that may have an anthropogenic origin.

In terms of the relationship between the stream sediments' composition and the geological formations it can be concluded that the stream sediments associated to the PA formation have the highest background values (EBVs) of the variables Co, Cr, Mn, Ni, and V (first PCA mode), which explains the enrichment seen in association Co-Cr-V-Mn, which is consistent with the mineralogical analysis that consists mainly of pyroxene, plagioclase, potassium feldspar, and phyllosilicates [36,61]; the stream sediments collected associated with the CB formation show depletion in Mn and Zn, which is consistent with the results obtained for the analysis of rocks [36]; the majority of the samples of stream sediments that occur associated with the AS formation is enriched in As, Cd, Hg, and Mn and impoverished in Co-Cr-Cu-Ni association, probably because this geological formation is significantly weathered and consequently impoverished in primary minerals such as pyroxene and olivine, and enriched in secondary minerals, such as hematite, phyllosilicates, serpentine and zeolite [61]. The stream sediments associated with the Monte das Vacas formation are impoverished in Co-Cr-Ni-V. The alluvium samples are particularly enriched in Ni.

The high values of ERIs for some elements demonstrate that the Santiago stream sediments may have higher Co, Cr, Ni, Mn and V risks which are caused by its higher natural origin. Nickel has the highest ERI values. The occurrence of values greater than 1 in the ERI maps shows that, on average, the contents of the respective metals are above the permissive levels. The PEC, above which harmful effects are likely in sediment dwelling organisms, was found for Cr and Ni.

So, this study shows that Santiago stream sediments present high natural heavy metals concentration levels, and are a potential risk to human health, which should be of concern to scientists and the government, needing epidemiologic studies.

## Acknowledgments

## Author Contributions

Marina Cabral Pinto performed the sampling, the pre-analytical treatment of samples, and the statistical analysis. Maria M. V. G. Silva participated in the field work. Eduardo Ferreira da Silva, Paulo Melo-Gonçalves, and Carla Candeias participated in data analysis. Marina Cabral Pinto drafted the manuscript with collaboration of all authors and it was revised by all. All authors read and approved the final manuscript.

## Conflicts of Interest

The authors declare no conflict of interest.

## References

1. Siegel, F.R. *Environmental Geochemistry of Potentially Toxic Metals*; Springer: Berlin, Germany, 2002.
2. Pinto, M.M.S.C.; Silva, M.M.V.G.; Neiva, A.M.R. Pollution of water and stream sediments associated with the Vale de Abrutiga Uranium Mine, Central Portugal. *Mine Water Environ.* **2004**, *23*, 66–75.
3. Pinto, M.M.S.C.; Silva, M.M.V.G. Contemporary reviews of mine water studies in Europe—Portugal. In *Mine Water and the Environment*; Wolkersdorfer, C., Bowell, R., Eds.; Springer: Berlin, Germany, 2005; pp. 50–53.
4. Komatina, M.M. *Medical Geology: Effects of Geological Environments on Human Health*; Developments in Earth and Environmental Sciences 2; Elsevier Science: Amsterdam, The Netherlands, 2004.
5. Kozlowski, H.; JanickaKlosb, A.; Brasunb, J.; Gaggelli, E.; Valensinc, D.; Valensinc, J. Copper, iron, and zinc ions homeostasis and their role in neurodegenerativedisorders (metal uptake, transport, distribution and regulation). *Coord. Chem. Rev.* **2009**, *253*, 2665–2685.
6. Gorell, J.M.; Johnson, C.C.; Rybicki, B.A.; Peterson, E.L.; Kortsha, G.X.; Kortsha, G.G.; Richardson, R.J. Occupational exposure to manganese, copper, lead, iron, mercury and zinc and the risk of Parkinson's disease. *Neurotoxicology* **1999**, *20*, 239–248.
7. Zatta, P.; Lucchini, R.; van Rensburg, S.J.; Taylor, A. The role of metals in neurodegenerative processes: aluminum, manganese, and zinc. *Brain Res. Bull.* **2003**, *62*, 15–28.
8. Elsner, R.; Spangler, J. Neurotoxicity of inhaled manganese: Public health danger in the shower? *Med. Hypotheses* **2005**, *65*, 607–616.
9. Erikson, K.M.; Syversen, T.; Aschner, J.L.; Aschner, M. Interactions between excessive manganese exposures and dietary iron-deficiency in neurodegeneration. *Environ. Toxicol. Pharmacol.* **2005**, *19*, 415–421.
10. Schneider, J.S.; Decamp, E.; Koser, A.J.; Fritz, S.; Gonczi, H.; Syversen, T.; Guilarte, T.R. Effects of chronic manganese exposure on cognitive and motor functioning in non-human primates. *Brain Res.* **2006**, *1118*, 222–231.
11. Cersosimo, M.G.; Koller, W.C. The diagnosis of manganese-induced parkinsonism. *NeuroToxicology* **2006**, *27*, 340–346.
12. Santamaria, A.B.; Cushing, C.A.; Antonini, J.M.; Finley, B.L.; Mowat, F.S. State-of-the-science review: Does manganese exposure during welding pose a neurological risk? *J. Toxicol. Environ. Health* **2007**, *10*, 417–465.
13. Flyn, M.R.; Susi, P. Neurological risks associated with manganese exposure from welding operations—A literature review. *Int. J. Hyg. Environ. Health* **2009**, *212*, 459–469.

14. International Agency for Research on Cancer. *Chromium, Nickel and Welding*; IARC Monographs on the Evaluation of Carcinogenic Risks to Humans Volume 49; International Agency for Research on Cancer: Lyon, France, 1990.

15. Staessen, J.A.; Buchet, J.P.; Ginucchio, G.; Lauwerys, R.R.; Lijnen, P.; Roels, H.; Fagard, R. Public health implications of environmental exposure to Cadmium and Lead: An overview of epidemiological studies in Belgium. *J. Cardiovasc. Risk* **2007**, *3*, 26–41.

16. Schroeder, H.A. Cadmium, chromium, and cardiovascular disease. *Circulation* **1967**, *35*, 570–582.

17. Panaullah, G.M.; Alam, T.; Baktear Hossain, M.; Loeppert, R.H.; Lauren, J.G.; Meisner, C.A.; Ahmed, Z.U.; Duxbury, J.M. Arsenic toxicity to rice (*Oryza sativa* L.) in Bangladesh. *Plant Soil* **2009**, *317*, 31–39.

18. Yao, Y.; Pei, F.; Kang, P. Selenium, iodine, and the relation with Kashin-Beck disease. *Nutrition* **2011**, *27*, 1095–1100.

19. Plant, J.A.; Smith, D.; Smith, B.; Williams, L. Environmental geochemistry at the global scale. *Appl. Geochem.* **2001**, *16*, 1291–1308.

20. Smith, D.B.; Smith, S.M.; Horton, J.D. History and evaluation of national-scale geochemical data sets for the United States. *Geosci. Front.* **2013**, *4*, 167–183.

21. Salminen, R.; Batista, M.J.; Bidovec, M.; Demetriades, A.; de Vivo, B.; de Vos, W.; Duris, M.; Gilucis, A.; Gregorauskiene, V.; Halamic, J.; *et al. Geochemical Atlas of Europe, Part 1: Background Information, Methodology and Maps*; Geological Survey of Finland: Espoo, Finland, 2005.

22. Johnson, C.C.; Breward, N.; Ander, E.L.; Ault, L. G-BASE: Baseline geochemical mapping of Great Britain and Northern Ireland. *Geochem. Explor. Environ. Anal.* **2005**, *5*, 347–357.

23. Garret, R.G.; Reimann, C.; Smith, D.B.; Xie, X. From geochemical prospecting to international geochemical mapping: A historical overview. *Geochem. Explor. Environ. Anal.* **2008**, *8*, 205–217.

24. Smith, D.B.; Reimann, C. Low-Density geochemical mapping and the robustness of geochemical patterns. *Geochem. Explor. Environ. Anal.* **2008**, *8*, 219–227.

25. Appleton, J.D.; Ridgway, J. Regional geochemical mapping in developing countries and its application to environmental studies. *Appl. Geochem.* **1993**, *2*, 103–110.

26. Xuejing, X.; Xuzhan, M.; Tianxiang, R. Geochemical mapping in China. *J. Geochem. Explor.* **1997**, *60*, 99–113.

27. Reimann, C.; Caritat, P. *Chemical Elements in the Environment—Factsheets for the Geochemist and Environmental Scientist*; Springer-Verlag: Berlin, Germany, 2008.

28. Lech, M.E.; Caritat, P. Regional Geochemical Study Paves Way for National Survey—Geochemistry of Near-Surface Regolith Points to New Resources. Available online: http://www.ga.gov.au/ausgeonews/ausgeonews200706/geochemical.jsp (accessed on 1 June 2007).

29. Inácio, M.; Pereira, V.; Pinto, M. The soil geochemical Atlas of Portugal: Overview and applications. *J. Geochem. Explor.* **2008**, *98*, 22–33.

30. Darnley, A. International geochemical mapping special issue. *J. Geochem. Explor.* **1990**, *39*, 1–13.

31. Darnley, A.G.; Björklund, A.; Bølviken, B.; Gustavsson, N.; Koval, P.V.; Plant, J.A.; Steenfelt, A.; Tauchid, M.; Xie, X. *A Global Geochemical Database for Environmental and Resource Management: Recommendations for International Geochemical Mapping*; Final Report of IGCP Project 259; UNESCO: Paris, France, 1995.

32. Albanese, S.; de Vivo, B.; Lima, A.; Cicchella, D. Geochemical background and baseline values of toxic elements in stream sediments of Campania region (Italy). *J. Geochem. Explor.* **2007**, *93*, 21–34.

33. Levinson, A.A. *Introduction to Exploration Geochemistry*; Applied Publishing Ltd.: Maywood, CA, USA, 1974.

34. Beus, A.A.; Grigorian, V. *Geochemical Exploration Methods for Mineral Deposits*; Applied Publishing Ltd.: Wilmette, IL, USA, 1977.

35. Reimann, C.; Siewers, U.; Tarvainen, T.; Bityukova, L.; Eriksson, J.; Gilucis, A.; Gregorauskiene, V.; Lukashev, V.K.; Matinian, N.N.; Pasieczna, A.; *et al. Agricultural Soils in Northern Europe: A Geochemical Atlas*; Schweizerbart Science Publishers: Stuttgart, Germany, 2003.

36. Cabral Pinto, M.M.S. Geochemical Cartography, with a Low To-Median Density, of Santiago Island, Cape Verde. Ph.D. Thesis, University of Aveiro, Aveiro, Portugal, 2010.

37. Desenfant, F.; Petrovský, E.; Rochette, P. Magnetic signature of industrial pollution of stream sediments and correlation with heavymetals: Case study from south France. *Water Air Soil Pollut.* **2004**, *152*, 297–312.

38. INE 2010. Censo 2010. Available online: http://www.ine.cv (accessed on 21 March 2013).

39. Serralheiro, A. A Geologia da ilha de Santiago (Cabo Verde). *Boletim Museu Laboratório Mineralógico Geológico Faculdade de Ciências de Lisboa* **1976**, *14*, 157–372. (In Portuguese)

40. Instituto Nacional de Meteorologia e Geofisica (INMG). *Climatologic Data of Some Stations in Santiago Island, Praia, Cabo Verde*; Internal Report; INMG: Praia, Santiago Island, Cabo Verde, 2005.

41. *United Nations Development Program for Cape Verde*; PNUD: New York, NY, USA, 1993.

42. Matos Alves, C.A.; Macedo, J.R.; Celestino Silva, L.; Serralheiro, A.; Peixoto Faria, A.F. Estudo geológico, petrológico e vulcanológico da ilha de Santiago (Cabo Verde). *Garcia de Orta Serviços Geológicos* **1979**, *3*, 47–74. (In Portuguese)

43. Ramalho, R.A.S. Building the Cape Verde Islands. Ph.D. Thesis, University of Bristol, Bristol, UK, 2011.

44. Holm, P.M.; Grandvuinet, T.; Friis, J.; Wilson, J.R.; Barker, A.K.; Plesner, P. An $^{40}$Ar-$^{39}$Ar study of the Cape Verde hot spot: Temporal evolution in a semistationary plate environment. *J. Geophys. Res.* **2008**, *113*, doi:10.1029/2007JB005339.

45. Pina, A.F.L. Hydrochemistry and groundwater quality of the island of Santiago, Cape Verde (Hidroquímica e qualidade das águas subterrâneas da ilha de Santiago, Cabo Verde). Ph.D. Thesis, University of Aveiro, Aveiro, Portugal, 2009. (In Portuguese)

46. Martins, S.; Mata, J.; Munhá, J.; Madeira, J.; Moreira, M. Evidências geológicas e geoquímicas para a existência de duas unidades estratigráficas distintas na Formação do Pico da Antónia (Ilha de Santiago, República de Cabo Verde). *Memórias e Notícias Universidade de Coimbra* **2008**, *3*, 123–128. (In Portuguese)

47. Rose, A.W.; Hawkes, E.H.; Webb, J.S. *Geochemistry in Mineral Exploration*, 2nd ed.; Academic Press: London, UK, 1979.

48. Thompson, M. Analytical methods in applied environmental geochemistry. In *Applied Environmental Geochemistry*; Thornton, I., Ed.; Academic Press: London, UK, 1983.

49. Chao, T.T.; Sanzolone, R.F. Decomposition techniques. *J. Geochem. Explor.* **1992**, *44*, 65–106.

50. Tukey, J.W. *Exploratory Data Analysis*; Addison-Wesley: Reading, UK, 1977.

51.  Reimann, C.; Filzmoser, P.; Garret, R.G.; Dutter, R. *Statistical Data Analysis Explained: Applied Environmental Statistics with R*, 1st ed.; John Wiley & Sons: Chichester, UK, 2008.

52.  Minister of the Environment (Canada). Soil, Ground Water and Sediment Standards for Use under Part XV.1 of the *Environmental Protection Act*. Available online: http://www.mah.gov.on.ca/AssetFactory.aspx?did=8993 (accessed on 15 April 2011).

53.  Italian Legislation: Decreto Ministeriale, n°471, 1999. Regolamento Recante Criteri, Procedure e Modalità per la Messa in Sicurezza, la Bonifica e il Ripristino Ambientale dei Siti Inquinati, ai Sensi Dell'artocolo 17 del Decreto Legislativo 5 Febbraio 1997, n.22, e Successive Modificazioni e Integrazioni; Gazzetta Ufficiale n°293 de 15 December 1999, Supplemento Ordinario n°218. Available online: http://www.eugris.info/FurtherDescription.asp?e=550&Ca=1&Cy=8&DocID=E&DocTitle=Management_administration&T=Italy (accessed on 15 October 2014). (In Italian)

54.  Sheng, J.; Wang, X.; Gong, P.; Tian, L.; Yao, T. Heavy metals of the Tibetan top soils—Level, source, spatial distribution, temporal variation and risk assessment. *Environ. Sci. Pollut. Res.* **2012**, *19*, 3362–3370.

55.  Ministry of Housing, Spatial Planning and the Environment (VROM). Circular on Target Values and Intervention Values for Soil Remediation. The Netherlands Government Gazette, No. 39, Ministry of Housing, Spatial Planning and Environment, Directorate General for Environmental Protection, Department of Soil Protection. Available online: http://www.esdat.net/Environmental%20Standards/Dutch/annexS_I2000Dutch%20Environmental%20Standards.pdf (accessed on 16 October 2014).

56.  Cannon, W.F.; Woodruff, L.G.; Pimley, S. Some statistical relationships between stream sediment and soil geochemistry in northwestern Wisconsin—Can stream sediment compositions be used to predict compositions of soils in glaciated terranes? *J. Geochem. Explor.* **2004**, *81*, 29–46.

57.  MacDonald, D.D.; Ingersoll, C.G.; Berger, T.A. Development and evaluation of consensus-based sediment quality guidelines for freshwater ecosystems. *Arch. Environ. Contam. Toxicol.* **2000**, *39*, 20–31.

58.  Smith, S.L.; MacDonald, D.D.; Keenleyside, K.A.; Ingersoll, C.G.; Field, J. A preliminary evaluation of sediment quality assessment values for freshwater ecosystems. *J. Gt. Lakes Res.* **1996**, *22*, 624–638.

59.  Persaud, D.; Jaagumagi, R.; Hayton, A. *Guidelines for the Protection and Management of Aquatic Sediment Quality in Ontario*; Water Resources Branch, Ontario Ministry of the Environment: Toronto, Canada, 1993.

60.  Environment Canada. *EC, MENVIQ (Environment Canada and Ministere de l'Envionnement du Quebec) Interim Criteria for Quality Assessment of St. Lawrence River Sediment*; Environment Canada: Ottawa, Canada, 1992.

61.  Cabral Pinto, M.M.S.; da Silva, E.A.F.; Silva, M.M.V.G.; Melo-Gonçalves, P. Estimated background values of some harmful metals in stream sediments of Santiago Island (Cape Verde). In *Geochemistry: Earth's System Processes*; Dionisios, P., Ed.; InTech: Rijeka, Croatia, 2012; pp. 61–80.